DOI: 10.4081/aiua.2025.14657

ORIGINAL PAPER

Biocompatibility and tissue integration of autologous fat grafts and synthetic implants following submucosal implantation into the urinary bladder

Meirambek Askarov [1], Ilona Pak [1], Dauren Yeskermessov [2], Ulpan Batenova [2], Dmitriy Klyuyev [2], Yevgeniy Kamyshanskiy [3], Min Sung Tak [4]

[1] Department of Surgical Diseases, Karaganda Medical University, Karaganda, Kazakhstan;
[2] Institute of Life Sciences, Karaganda Medical University, Karaganda, Kazakhstan;
[3] Head of the Pathological Anatomy Unit of the Clinic of Karaganda Medical University, Karaganda, Kazakhstan;
[4] Department Plastic Surgery, Soon Chun Hyang University Cheonan Hospital, Cheonan, South Korea.

Summary ***Background:*** *In urological practice, the search continues for volume-forming materials with optimal biocompatibility, a prolonged therapeutic effect, and a minimal risk of complications. This issue is particularly critical in reconstructive and functional urology, where long-term stability of the outcome is required without inducing damage to the surrounding tissues. Existing synthetic and biological fillers present several limitations, including a tendency toward resorption, fibrosis, shape instability, and the risk of immune reactions. Although the efficacy of certain materials has been demonstrated, issues related to their long-term biocompatibility and morpho-functional stability remain unresolved.*

Methods: *Ninety-six sexually mature male Belgian rabbits were used in the experiment. Under intravenous anesthesia, a submucosal injection of the volume-forming material (0.3 mL) was administered into the wall of the urinary bladder. Four types of materials were employed in the study: autologous fat graft, autologous fat graft combined with platelet-rich plasma (PRP), poly-L-lactic acid (aesPLLa), and macroparticles of a polyacrylate-polyvinyl alcohol copolymer. Animals were divided into four experimental groups according to the type of material administered. To assess tissue responses and graft characteristics, subgroups of eight animals from each experimental group were euthanized on days 14, 30, and 90 post-intervention for comprehensive morphological evaluation, including histological, histochemical, histomorphometric, and morphometric analyses.*

The primary evaluation parameters included the intensity of the inflammatory response, the degree of vascularization, the nature of cellular infiltration, the extent of fibrotic changes, and the preservation of the implanted material.

Results: *The study demonstrated that the combination of an autologous fat graft with platelet-rich plasma (PRP) promoted more intensive microvascular network formation, reduced inflammatory infiltration, and ensured a more uniform distribution of the transplanted tissue compared with the other experimental groups. The obtained data indicate the high biocompatibility of this combination and its potential effectiveness as an alternative to synthetic volume-forming materials, particularly in clinical settings requiring a prolonged volumetric effect with minimal risk of complications.*

Conclusions: *The combination of platelet-rich plasma (PRP) with an autologous fat graft, as well as the use of the synthetic material polyacrylate and polyvinyl alcohol copolymer, appear to be the most promising approaches for achieving a stable and biocompatible volume-forming effect in the correction of lower urinary tract pathologies. At the same time, despite the confirmed high biocompatibility of the investigated substrates in the short term, questions regarding their long-term safety remain unresolved, including the risk of fibrotic changes and potential functional impairments of the urinary bladder. These aspects warrant further investigation and clinical validation.*

KEY WORDS: Lipofilling; Platelet-rich plasma (PRP); Uroimplant; Filler; Vesicoureteral reflux.

Submitted 15 November 2025; Accepted 25 November 2025

INTRODUCTION

Volume-forming fillers play a key role in the surgical management of a wide range of urological disorders. In the context of growing interest in minimally invasive therapeutic approaches, the choice between synthetic and autologous materials has become particularly significant (1-4). Current evidence indicates that autologous substrates possess several advantages over synthetic analogs, particularly in terms of biocompatibility, their ability to stimulate tissue regeneration, and to maintain long-term clinical efficacy (5-7). At the same time, a comprehensive comparative evaluation of these materials in urological practice is presented in the literature only fragmentarily and requires further in-depth investigation. Modern uroimplants are classified into natural (autologous) and synthetic materials. Natural substrates include biological agents such as fibroblasts, plasma clots, adipocytes, chondrocytes, as well as human collagen and bovine dermal collagen. Among synthetic materials, the most widely used are polytetrafluoroethylene (*Teflon paste*), polydimethylsiloxane (*Macroplastique*), polyacrylamide hydrogel (*DAM+, Interfall, Formacryl*), dextranomer-hyaluronic acid copolymers (*Urodex, Deflux*), and macroparticles of polyacrylate-polyvinyl alcohol copolymer (*Vantris*).

The primary criterion determining the clinical effectiveness of volume-forming implants is their stability that is the the ability to maintain the initial volume over an extended period after administration. Instability has been observed in several synthetic materials (such as polytetrafluoroethylene, polydimethylsiloxane, polyacrylamide hydrogel, and polyacrylate-polyvinyl alcohol macroparticles), as well as in certain biological substrates (including collagen, chondrocytes, and adipocytes) (8).

The experience gained from the use of various fillers in pediatric urology, particularly in the correction of vesicoureteral reflux, has made it possible to define the fundamental requirements for their physicochemical and biological properties. In addition, volume-forming agents have been applied in the treatment of stress urinary incontinence (9), postcoital cystitis (10), Peyronie's disease (11, 12), as well as in procedures aimed at penile augmentation (13).

Thus, despite the accumulated clinical experience and the wide range of available solutions, urological practice still lacks a unified protocol for selecting the optimal volume-forming material that would meet all key criteria: volume stability, absence of migration, preservation of morphological and histological patterns, high biocompatibility, availability, and safety of use.

This fact underscores the need for further comprehensive comparative studies of synthetic and autologous materials, which determines the relevance of the present study.

Materials and methods

Study design

Animal care and housing conditions during the experimental period were in accordance with relevant international and national guidelines (14-16).

The sample size was determined using the Monte Carlo method with Markov chains (17), taking into account the availability of animals in the university medical vivarium, the justified increase in the number of experimental cases, and ethical considerations aimed at minimizing the use of animals in research.

A total of 96 laboratory animals were randomly enrolled in the experimental study and allocated into four equal groups, each comprising 24 subjects. All animals underwent the administration of volume-forming substrates into the submucosal layer of the urinary bladder wall. The allocation of animals into groups was carried out as follows:

- Group I (autologous fat graft) – administration of autologous adipose tissue.
- Group II (autologous fat graft + PRP) – combined administration of autologous adipose tissue and *platelet-rich plasma* (PRP).
- Group III (polylactic acid, aesPLLa) – administration of a preparation based on poly-L-lactic acid.
- Group IV (*Vantris*) – administration of macroparticles composed of a polyacrylate and polyvinyl alcohol copolymer (*Vantris*).

The study design is presented in Figure 1.

Animals

As experimental subjects, 96 male Belgian Flanders rabbits aged 6 months and weighing 4.5-5.0 kg were used. The animals were housed individually in separate cages under controlled sanitary and hygienic conditions at a temperature of 22 ± 2°C, with a 12-hour light/dark cycle and relative humidity of not less than 40%. The rabbits were fed a standard pelleted diet, with free access to water ad libitum.

Method for the preparation of PRP

PRP was obtained using a two-step centrifugation method. For this purpose, 3 mL of peripheral blood collected from the marginal ear vein of the rabbit was added to a 9 mL test tube containing 1 mL of heparin. The first centrifugation step was performed at 1700 g for 10 minutes. Afterward, the intermediate layer containing platelet-rich plasma was separated and subjected to a second centrifugation at 800 g for 10 minutes to isolate the PRP pellet from the platelet-poor plasma. As a result, PRP with a platelet concentration of approximately 1.2 × 10^8 cells/mL was obtained (18).

Surgical procedures

All experimental animals (rabbits) underwent identical surgical procedures, which included preoperative preparation, general anesthesia, and the intervention itself, performed in accordance with established standards of asepsis and antisepsis.

General anesthesia was induced using a combination of tiletamine/zolazepam at a dose of 20 mg/kg and xylazine at a dose of 3 mg/kg administered intramuscularly, followed by supplemental oxygen delivery (19). After achieving adequate anesthesia, the animal was positioned supine and urinary bladder catheterization was performed.

Lipoaspirate for autotransplantation was harvested from the inguinal region using cannulas equipped with one central and two lateral openings, with an internal diameter of 3.0 mm for both the cannula and each opening (20). The submucosal layer of the anterior wall of the urinary bladder was selected as the recipient site. A volume-forming substrate (0.3 mL) was administered as a bolus injection using a 22G needle. All procedures were performed by the same surgeon to minimize interventional variability.

Figure 1.
Study design.

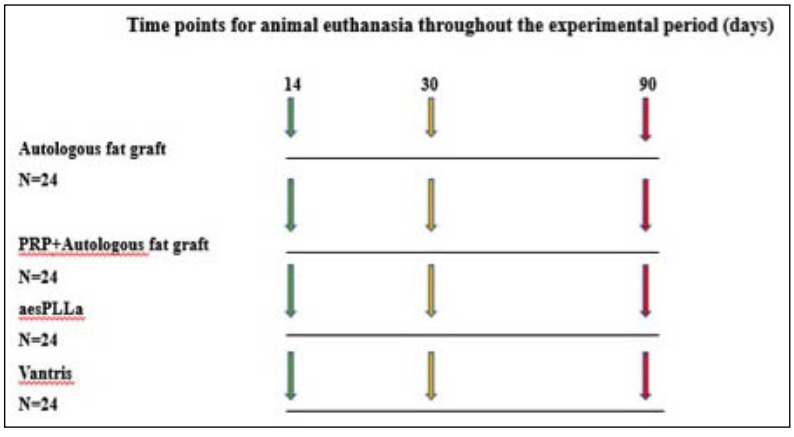

Animals were euthanized on days 14, 30, and 90 post-procedure, with eight rabbits from each experimental group sacrificed at each designated time point. Each animal was euthanized using a combined anesthetic protocol involving tiletamine/zolazepam and xylazine, followed by administration of a barbiturate to ensure complete termination in accordance with institutional and veterinary ethical guidelines. Tissue samples were collected for comprehensive morphological evaluation, including histological, histochemical, and histomorphometric analyses.

Histological analysis

Preparation of biological material

The study material consisted of bladder tissue fragments containing the site of biomaterial implantation. The tissues were fixed in 10% neutral buffered formalin at 4°C for 24 hours. The samples were labeled with the animal identification number and date, without indication of the experimental group (I – autologous fat graft, II – autologous fat graft with PRP, III – aesPLLa, IV – polyacrylate and polyvinyl alcohol copolymer).

After fixation, the tissues were rinsed, dehydrated in alcohols, cleared in xylene, and embedded in paraffin. Sections 3-4 μm thick were cut using a microtome, stained with hematoxylin, eosin, and Masson's trichrome, mounted with a coverslip, and examined under a light microscope.

Histochemical analysis

Masson's trichrome staining

Masson's trichrome staining was performed using a commercially available kit (*Trichrome Stain [Masson], Biovitrim TU 9398-001-89079081-2012*) following the standard protocol. Masson's trichrome was used to identify fibrous tissue and blood vessels. This staining method colors mature type I collagen dark blue.

Histomorphometric assessment

Biocompatibility assessment was carried out in accordance with the guidelines outlined in Biological Evaluation of Medical Devices - Part 6: Tests for Local Effects After Implantation (ISO/DIS 10993-6:2024) (21). Histological analysis was based on a semi-quantitative scale that enabled the evaluation of structural and inflammatory alterations in the bladder tissues, including the epithelium, lamina propria, muscular layer, and the capsule surrounding the implant. Each parameter was assessed using a semi-quantitative scoring system adapted for reproducibility and comparative analysis, in accordance with the standards of ISO/DIS 10993-6:2024 (21).

Epithelium

Structural integrity

Evaluation of epithelial morphological alterations:

0 - normal (multilayered transitional epithelium with a well-defined cellular organization and no evidence of structural damage);
1 - mild alterations (limited areas of desquamation and/or localized thinning or hyperplasia of the epithelium, with preservation of overall stratification);
2 - moderate alterations (superficial desquamation of the epithelial layer, moderate hyperplasia or thinning of the basal layer, and partial disruption of intercellular junctions);
3 - severe alterations (erosions with complete loss of the superficial epithelial layers down to the basement membrane and/or pronounced diffuse thinning and/or marked hyperplasia).

Cellular composition and organization

Histopathological alterations were evaluated based on the degree of disruption of cellular stratification and the severity of dystrophic changes:

0 - normal (well-defined cellular stratification, no evidence of dystrophy);
1 - mild alterations (partial loss of stratification with the appearance of occasional vacuolated cells);
2 - moderate alterations (pronounced vacuolization, focal dystrophic changes, and localized loss of stratification);
3 - severe alterations (destruction of epithelial layers, complete loss of normal stratification, and marked cellular dystrophy with morphological features of degeneration).

Inflammation

The degree of inflammatory cell infiltration was evaluated by quantifying various cell types:

Polymorphonuclear neutrophils, lymphocytes, and plasma cells

Were counted in five randomly selected high-power fields (×200):

0 - no inflammatory cells detected;
1 - mild infiltration (1-5 cells);
2 - moderate infiltration (6-10 cells);
3 - severe infiltration (more than 10 cells).

Multinucleated giant cells and eosinophils

Were counted in five randomly selected high-power fields (×200):

0 - no inflammatory cells detected;
1 - mild infiltration (1-2 cells);
2 - moderate infiltration (3-5 cells);
3 - severe infiltration (more than 5 cells).

Metaplasia

Metaplasia was determined based on changes in the cellular phenotype:

No, n (%): transitional epithelium without signs of transformation; the number of cases without evidence of dysplasia or atypia is indicated.

Yes, n (%): partial or diffuse replacement of the transitional epithelium by stratified squamous epithelium; the number of cases showing signs of dysplasia or atypia is indicated.

Dysplasia or atypia

Yes, n (%): number of cases showing signs of dysplasia or atypia.

No, n (%): number of cases without signs of dysplasia or atypia.

Lamina propria

Fibrosis

The degree of collagen fiber proliferation was evaluated as follows:

0 - normal (loose connective tissue without signs of excessive collagen deposition);
1 - mild changes (slight fibrosis characterized by sparse collagen fibers with focal condensation occupying < 10% of the area);
2 - moderate changes (thickened collagen fibers and moderate fibrosis involving 10-30% of the area);
3 - severe changes (dense collagen bundles, hyalinization, and pronounced fibrosis involving > 30% of the area).

Vascularization
The number and distribution of blood vessels were evaluated in five randomly selected fields at ×40 magnification:
0 - normal vessel density with uniform distribution;
1 - minimal alterations, occasionally dilated vessels grouped in small clusters (2-3 vessels) with uneven distribution;
2 - moderate alterations, dilated vessels forming clusters of 4-7 vessels;
3 - marked increase in capillary density with broad vascular bands.

Inflammation
Polymorphonuclear neutrophils, lymphocytes, and plasma cells
Were counted in five randomly selected high-power fields (×200):
0 - no inflammatory cells detected;
1 - mild infiltration (1-5 cells);
2 - moderate infiltration (6-10 cells);
3 - severe infiltration (more than 10 cells).

Multinucleated giant cells and eosinophils
Were counted in five randomly selected high-power fields (×200):
0 - no inflammatory cells detected;
1 - mild infiltration (1-2 cells);
2 - moderate infiltration (3-5 cells);
3 - severe infiltration (more than 5 cells).

Muscular layer
Fibrosis and sclerosis
Evaluation was performed based on the thickness and extent of collagen bands:
0 - normal (well-organized muscle fibers with collagen septa occupying ≤10% of the area);
1 - sclerosis (ingrowth of connective tissue between muscle fibers involving 10-30% of the muscular layer area);
2 - fibrosis (replacement of muscle tissue with dense fibrous connective tissue involving >30-50% of the area);
3 - scarring (deep structural alterations of the muscular layer involving >50% of the area, with foci of hyalinization and dystrophic changes).

Inflammation
The degree of inflammation was assessed using a semi-quantitative method:
0 - no inflammatory cells detected;
1 - mild infiltration by lymphocytes and macrophages (≤5 cells in five high-power fields, ×200);
2 - moderate infiltration by lymphocytes, macrophages, and plasma cells (>10 cells in five high-power fields, ×200);
3 - acute inflammation characterized by a predominant neutrophilic infiltrate (>10 cells in five high-power fields, ×200).

Capsule surrounding the implant
Capsule thickness
It was evaluated using a semi-quantitative method according to the following scale:
0 - capsule absent or very thin;
1 - moderately developed capsule;
2 - thick capsule;
3 - hypertrophic capsule.

Cellular composition
The cellular composition of the capsule was assessed semi-quantitatively according to the following scale:
0 - single fibroblasts, no inflammatory cells;
1 - fibroblasts and occasional macrophages (≤5 cells in five high-power fields at ×200 magnification);
2 - fibroblasts, macrophages, and lymphocytes (6-20 cells in five high-power fields at ×200 magnification);
3 - dense infiltration of fibroblasts, macrophages, and lymphocytes, with possible presence of plasma cells (>20 cells in five high-power fields at ×200 magnification).

Fibrosis and collagen density
Fibrosis and collagen density were assessed semi-quantitatively according to the following scale:
0 - loose collagen fibers without thickening;
1 - sparse collagen with focal fiber thickening;
2 - dense collagen bundles with intense Masson's trichrome staining and pronounced fiber thickening;
3 - marked fibrosis with collagen hyalinization.

Inflammation
Inflammatory response was evaluated semi-quantitatively according to the following scale:
0 - absence of inflammatory cells;
1 - mild infiltration with lymphocytes and macrophages (≤5 cells in 5 high-power fields, ×200);
2 - moderate infiltration with lymphocytes, macrophages, and plasma cells (>10 cells in 5 high-power fields, ×200);
3 - acute inflammation characterized by a neutrophilic infiltrate (>10 cells in 5 high-power fields, ×200).

Foreign Body Giant Cell Reaction
The giant cell response was evaluated semi-quantitatively according to the following scale:
0 - no multinucleated giant cells observed;
1 - rare giant cells (1-4 cells in 5 high-power fields, ×200);
2 - moderate number of giant cells (>5 cells in 5 high-power fields, ×200);
3 - numerous giant cells forming continuous fields at ×200 magnification.

Statistical analysis
Quantitative data obtained from histological, histochemical, and morphometric evaluations – including parame-

ters of inflammatory response, vascularization, cellular infiltration, fibrosis, and implant integrity – were subjected to statistical analysis. All datasets were tested for normality using the Shapiro-Wilk test. Since the data followed a normal distribution, statistical comparisons were performed using one-way *analysis of variance* (ANOVA), followed by Tukey's post hoc test for multiple group comparisons. Results are expressed as *mean ± standard deviation* (M ± SD). Pearson's correlation analysis was applied to assess the relationships between key morphological parameters (vascular density, fibrosis intensity, and implant degradation). Linear regression analysis was performed to evaluate the association between inflammatory activity and implant stability over time. All statistical analyses were carried out using SPSS Statistics 25.0 (*IBM Corp., Armonk, NY, USA*) and R Studio (version 4.3.0). Differences were considered statistically significant at $p < 0.05$.

Ethical considerations

The protocol for the blinded randomized in vivo study was approved by the *Bioethics Committee of the Non-profit Joint Stock Company "Karaganda Medical University" (Protocol No. 91, dated December 3, 2024)*. All experimental procedures were conducted in accordance with the ethical principles for animal research and under the supervision of a certified veterinarian to prevent any unnecessary pain, distress, or suffering throughout the study.

Results

Autologous Transplants (Autologous Fat Graft and PRP + Autologous Fat Graft), Day 14

Autologous Fat Graft

After 14 days from implantation of autologous adipose tissue into the bladder wall, pronounced resorption of the graft with replacement by fibrous tissue was observed (Figure 2). In 50 % of the samples (4 of 8), mild dystrophic changes characterized by cytoplasmic vacuolization and slight lymphocytic infiltration were detected. The implantation site exhibited the formation of fat cysts accompanied by a marked inflammatory response.

In the lamina propria, moderate fibrosis (1.5 points), pronounced lymphocytic infiltration (3 points), and accumulation of multinucleated giant cells (3 points) were recorded. The inflammatory infiltrate consisted of neutrophils (1 [0.75-1]), eosinophils (1 [1-1]), lymphocytes (3 [3-3]), and macrophages (3 [2.75-3]).

The muscular layer was largely preserved, showing only isolated areas of fibrosis and sclerosis (0-1 point) without signs of inflammation.

In all samples (8 of 8), a connective tissue capsule had formed around the graft, demonstrating pronounced fibrotic remodeling: capsule thickness (2 [2-3] points), collagen fiber density (2 [2-2.25] points), with infiltration by fibroblasts, macrophages, and lymphocytes. The multinucleated giant cell reaction reached 3 points, indicating active degradation of the implanted graft.

Figure 2.
Autologous fat graft at day 14.

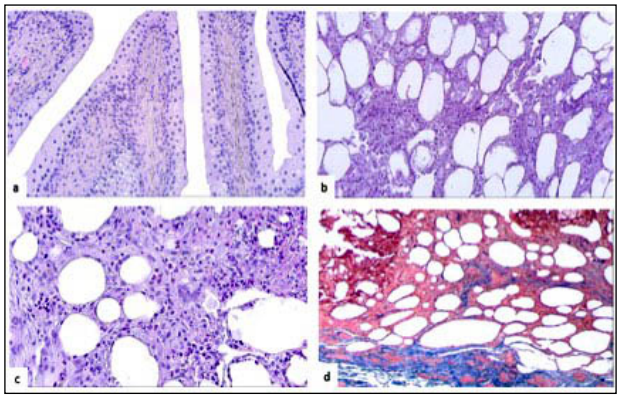

PRP + Autologous Fat Graft

At 14 days after implantation, partial remodeling of the graft was observed, characterized by moderate vascularization and minimal inflammatory response (Figure 3). The urothelium appeared normal in 75% of cases (6 out of 8), while in 25% of samples, mild dystrophic changes and occasional inflammatory elements were noted. In isolated sections, slight epithelial hyperplasia and vacuolization were detected, without signs of dysplasia or metaplasia.

Figure 3.
PRP-enhanced autologous fat graft at day 14.

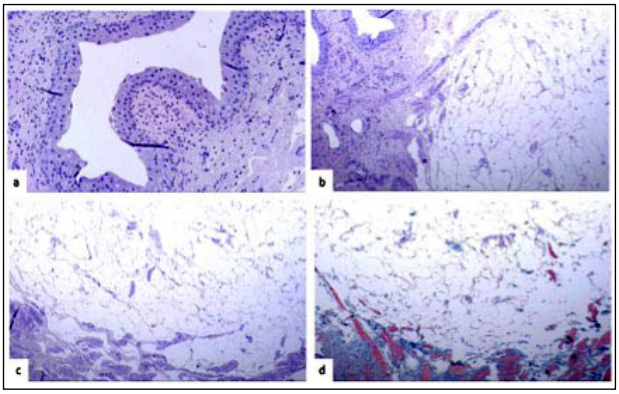

In the lamina propria, moderate thickening of collagen fibers (0.5 points) and increased vascularization (1.5 points) were recorded, reflecting early fibrotic remodeling and reestablishment of the vascular network. The inflammatory response was mild, with limited infiltration by individual lymphocytes and plasma cells (1-2 points). Multinucleated giant cells were rarely observed (1-1.25 points).

The muscular layer retained an intact structure without signs of inflammation, fibrosis, or sclerosis; smooth muscle fibers exhibited an orderly arrangement, and nuclei were evenly distributed.

A fibrous capsule was formed in all samples (8 out of 8), with moderate thickness (1 [1-2] points) and cellular infiltration by fibroblasts, macrophages, and lymphocytes (2 points). The capsule structure corresponded to moderately dense connective tissue without evidence of scarring. Inflammatory changes within the capsule were mild

(1.5 [1-2] points), and the multinucleated giant cell reaction was rated at 2 points, indicating gradual graft degradation with minimal phagocytic activity.

Autologous Transplants (Autologous Fat Graft and PRP + Autologous Fat Graft), Day 30

Autologous Fat Graft

After 30 days from graft implantation into the bladder wall, pronounced signs of adipose tissue resorption and active fibrotic remodeling were observed (Figure 4). The urothelium remained morphologically intact in all samples (100%), with a normal cellular composition in 75% of cases and minor dystrophic changes and vacuolization in 25%.

Adipose tissue exhibited marked destruction, with cyst formation and pronounced inflammatory infiltration. In the lamina propria, mild to moderate fibrosis (2-3 points) was noted, accompanied by markedly reduced vascularization (0-0.25 points), indicating low angiogenic activity. The inflammatory infiltrate consisted mainly of lymphocytes, macrophages, and multinucleated giant cells (3 points).

Within the graft area, small to medium-sized cysts predominated, along with enlarged and deformed adipocytes interspersed with cells of normal morphology. In most microscopic fields, adipocytes with disrupted architecture prevailed; cells retaining a typical structure (a single large lipid droplet displacing the cytoplasm and nucleus peripherally) were rare.

The muscular layer preserved its structural integrity: smooth muscle fibers remained continuous and well-organized, without signs of inflammation or fibrosis.

A fibrous capsule surrounding the graft was identified in all specimens (8 out of 8). Its average thickness was 2 (1-2) points; the capsule exhibited a dense structure with moderate cellular infiltration (1 [1-2] points), predominantly by fibroblasts and macrophages. Masson's trichrome staining revealed mature, organized fibrous and fibrovascular tissue (2 [2-3.25] points): collagen fibers of variable thickness appeared wavy and irregularly oriented, with flattened cells and vascular bundles arranged parallel to the fibers.

The collagen fiber density corresponded to 1 (0.75-1) point, indicating a moderate degree of collagenization

Figure 4.
Autologous fat graft at day 30.

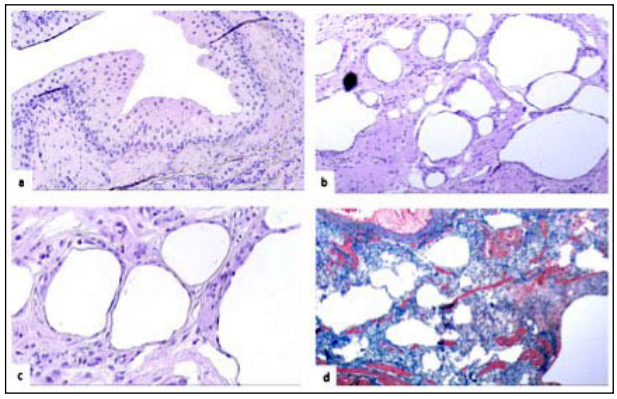

associated with graft resorption and replacement by connective tissue. In several samples, the inflammatory response within the capsule was attenuated, reflecting completion of the active immune phase. The multinucleated giant cell reaction persisted at a moderate level (1.5 [1-2] points) suggesting ongoing but less intense graft degradation.

PRP + Autologous Fat Graft, Day 30

At 30 days after implantation, active degradation of adipose tissue was observed, followed by its replacement with dense connective tissue (Figure 5). The epithelial layer remained intact in all cases; only one specimen (12.5%) exhibited mild dystrophic changes.

In the implantation zone, morphologically preserved adipose tissue predominated, represented by adipocytes of uniform shape and size, with focal areas of cystic degeneration, vacuolization, and localized proliferation of connective tissue. Isolated fibrous strands with signs of myxoid degeneration (0.5 [0-1] points) were identified. Cystic formations were surrounded by inflammatory infiltrates composed of macrophages, lymphocytes, and multinucleated giant cells, accompanied by the development of cystic cavities characteristic of steatonecrosis.

A fibrous capsule was formed in all samples (8 out of 8) and was characterized by moderate density and inflammatory activity, reflecting controlled yet active tissue remodeling. The multinucleated giant cell response was also moderate, indicating macrophage-mediated immune involvement without pronounced phagocytic activity.

Figure 5.
PRP-enhanced autologous fat graft at day 30.

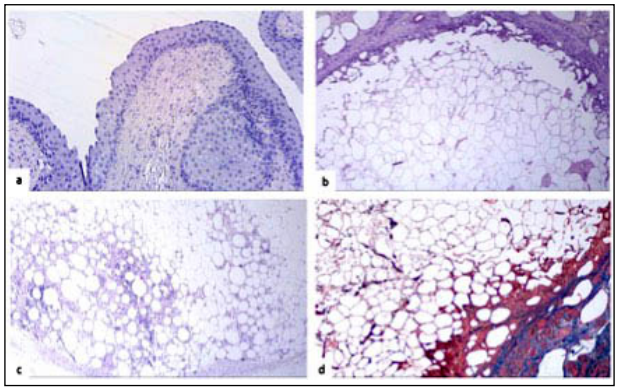

Autologous Transplants (Autologous Fat Graft and PRP + Autologous Fat Graft), Day 90

Autologous Fat Graft

At 90 days after implantation of the autologous fat graft into the bladder wall, almost complete resorption of the graft was observed, accompanied by its replacement with fibrous tissue (Table 1, Figure 6). The epithelial layer remained intact in all specimens (100%) without evidence of erosion, metaplasia, inflammation, or pronounced dystrophic changes; only mild cytoplasmic vacuolization was detected in 3 out of 8 samples (37.5%).

In the lamina propria, collagen fibers were distributed unevenly, forming focal accumulations. The degree of

Figure 6.
Autologous fat graft at day 90.

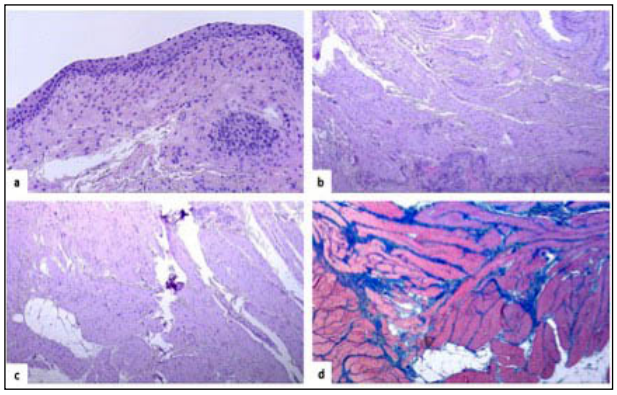

fibrosis averaged 2-2.25 points, reflecting moderate replacement of the resorbed graft with connective tissue. In the former implantation zone, inflammatory response was minimal, consisting of scattered lymphocytes and occasional multinucleated giant cells.
The muscular layer remained intact, without destructive changes, sclerosis, or inflammatory infiltration. Smooth muscle fibers preserved normal morphology and orientation, indicating the absence of adverse effects of the graft on the deeper layers of the bladder wall.
A fibrous capsule was present in most cases, with an average thickness of 2 (1.75-2) points. In one specimen (12.5%), the capsule was not detected, likely due to complete graft resorption. Fibrosis and collagen density were also estimated at 2 (1.75-2) points, suggesting stable yet moderate connective tissue remodeling without evidence of pathological scarring. Thus, by day 90, almost complete resorption of the graft was observed, accompanied by the formation of mature fibrous tissue and preservation of normal epithelial morphology.

PRP + Autologous Fat Graft, Day 90

At 90 days after implantation of the PRP-autologous fat graft, successful integration of the graft with the surrounding tissues was observed, along with preservation of normal histoarchitecture and minimal inflammatory response (Table 1, Figure 7). The epithelium remained intact in all specimens (100%), without signs of destruction, dysplasia, metaplasia, or inflammatory infiltration. Pronounced dystrophic changes or cytoplasmic vacuolization were not detected.
In the lamina propria, moderate fibrosis was noted, characterized by a uniform distribution of collagen fibers without thickening or focal accumulations. Vascularization was scored at 1 (0.75-1) point, indicating preserved yet moderate blood supply in the implantation zone. The inflammatory response was minimal, consisting of isolated lymphocytes and occasional multinucleated giant cells (1 point), reflecting the resolution phase of the immune reaction.
The muscular layer maintained morphological integrity and an orderly arrangement of smooth muscle fibers, with no evidence of inflammation or fibrosis, confirming the high biocompatibility of the graft and the absence of adverse effects on the deeper bladder wall layers.
A fibrous capsule was identified in all samples (100%), with an average thickness of 1 (1-1.25) point, corresponding to a thin, well-organized connective tissue structure. Collagen fiber density was estimated at 2 (1-2) points, without signs of pronounced sclerosis. The multinucleated giant cell reaction was rated at 1-1.25 points, indicating residual macrophage activity.
Thus, by day 90, the PRP-autologous fat graft demonstrated a high degree of biocompatibility and stable integration, accompanied by minimal inflammation and moderate tissue remodeling.

Synthetic Biomaterials (aesPLLa, polyacrylate and polyvinyl alcohol copolymer), Day 14

aesPLLa

At 14 days after implantation of the polylactic acid-based biomaterial (aesPLLa) into the rabbit bladder wall, only minimal changes in the urothelium were observed (Figure 8). In 75% of cases, focal epithelial thinning was noted, and in 50%-mild dystrophic alterations, including partial loss of nuclear stratification and cytoplasmic vacuolization of individual cells. The mean epithelial alteration score was 0.5 (0-1), while the urothelial histoarchitecture remained preserved. No signs of metaplasia, dysplasia, or cellular atypia were detected.
The immune response was mild: occasional neutrophils and eosinophils were observed in 37.5% of specimens, while lymphocytes and plasma cells were present in small

Figure 7.
PRP-enhanced autologous fat graft at day 90.

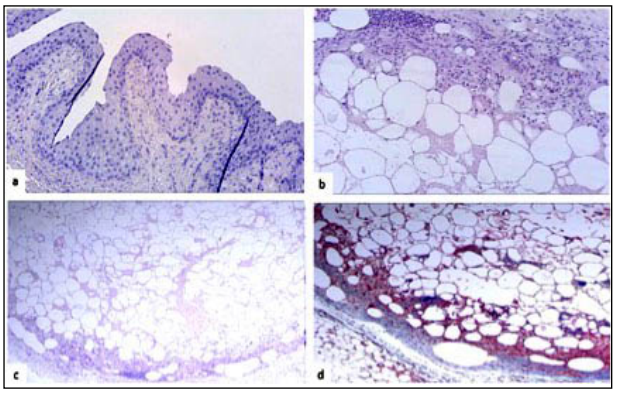

Figure 8.
aesPLLa group at day 14.

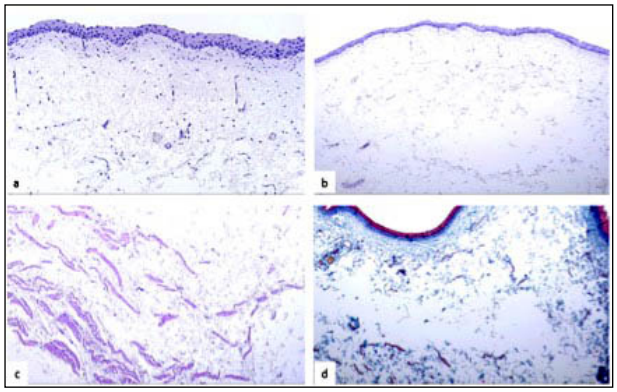

numbers (0.5 [0-1] points). In the lamina propria, moderate edema and loosening of connective tissue were evident, without signs of collagen disorganization. Masson's trichrome staining revealed thin, uniformly distributed collagen fibers without thickening, hyalinization, or fibrotic changes. Occasional thin-walled vessels were present.
Fragments of aesPLLa were diffusely distributed within the intercellular matrix without aggregation or conglomerate formation. Immune cell infiltration in the implantation zone was minimal (1 [0-1.25] points), with no evidence of pathological reaction. The muscular layer maintained its normal architecture: smooth muscle fibers were regularly arranged, with oval nuclei showing no hyperchromasia or karyopyknosis. Fine interstitial collagen fibers were present between muscle bundles without thickening, and no inflammatory cells were detected.
In all samples (100%), no fibrous capsule formation was observed around the aesPLLa fragments. Collagen fibers were evenly distributed, and no signs of hyalinization or fibrosis were noted. Multinucleated giant cells were absent, indicating high biocompatibility of the material and the absence of a pronounced cellular reaction.

Polyacrylate and polyvinyl alcohol copolymer, Day 14
At 14 days after implantation of Vantris, the urothelial structure remained preserved in 75% of cases, while mild focal hyperplasia was observed in 25% (0 [0-0.3] points) (Figure 9). In 37.5% of samples, signs of impaired stratification and vacuolization of urothelial cells were noted, though the overall histoarchitecture remained intact (0 [0-1] points). No infiltration of immune cells within the epithelium was observed. Metaplasia, dysplasia, and cellular atypia were absent.
The lamina propria consisted of loose connective tissue without signs of fibrosis. Immune cell infiltration was minimal, represented by single lymphocytes and plasma cells evenly distributed throughout the tissue. Isolated multinucleated giant cells were detected around individual implant fragments, indicating the onset of degradation processes accompanied by a mild inflammatory response.
The muscular layer retained its normal morphology: smooth muscle fibers were orderly arranged, with no evidence of dystrophy, inflammation, or sclerosis. Thin, evenly distributed collagen fibers were present between muscle bundles without thickening.
A fibrous capsule was formed in all samples (100%), clearly demarcating the implant from the surrounding tissues. Collagen fibers within the capsule exhibited an organized orientation, forming parallel bundles. The capsule demonstrated moderate thickness, with areas of loose collagen and focal fiber thickening. The inflammatory and giant-cell reactions did not exceed 1 point, confirming the high biocompatibility of the material and the absence of a pronounced immune response.

Figure 9.
Vantris group at day 14.

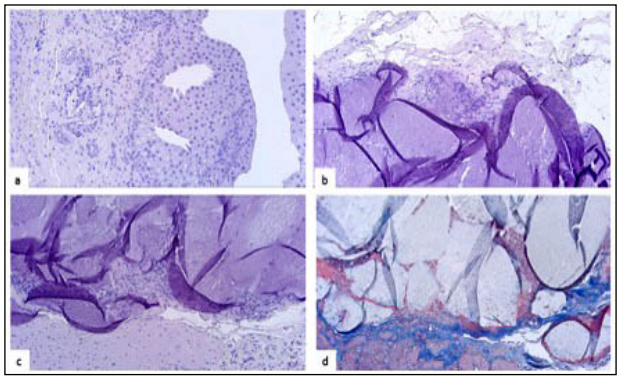

aesPLLa, Day 30
At 30 days after implantation of aesPLLa, histological examination revealed pronounced epithelial damage in all samples (Figure 10). Severe alterations were observed in 100% of cases, including desquamation, thinning, hyperplasia, and erosion (2.5 [2.0-3.0] points). Cellular organization was disrupted, with evident stratification disorders, dystrophy, and vacuolization (1.5 [1-2] points). The urothelium exhibited diffuse eosinophilic infiltration (3 points), accompanied by scattered lymphocytes and occasional plasma cells (0.5 [0-1] points). Metaplasia, dysplasia, and cellular atypia were not detected.

Figure 10.
aesPLLa group at day 30.

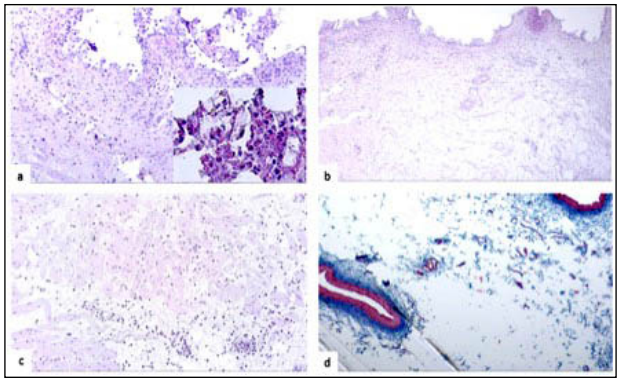

The lamina propria corresponded to normal histological architecture and consisted of loose fibrous connective tissue. Infiltration by lymphocytes, plasma cells, and eosinophils was primarily localized to the subepithelial region.
The muscular layer preserved its normal morphology: smooth muscle fibers were arranged in an orderly fashion, without evidence of dystrophy, fibrosis, or inflammatory infiltration.
Formation of a fibrous capsule was not observed in any of the specimens. Collagen fibers were evenly distributed, without focal accumulations or signs of connective tissue remodeling. No inflammatory or multinucleated giant-cell reactions were detected, suggesting partial metabolic inertness of the material despite its epithelial toxicity.

Polyacrylate and polyvinyl alcohol copolymer, Day 30
At 30 days after implantation of Vantris, the urothelial structure remained within normal limits in 50% of the animals, while the remaining cases demonstrated minimal alterations, including focal epithelial thinning and parabasal hyperplasia (0.5 [0-1] points), as well as mild stratification disturbances, cellular dystrophy, and vacuolization (0 [0-1] points) (Figure 11). No evidence of

Figure 11.
Vantris group at day 30.

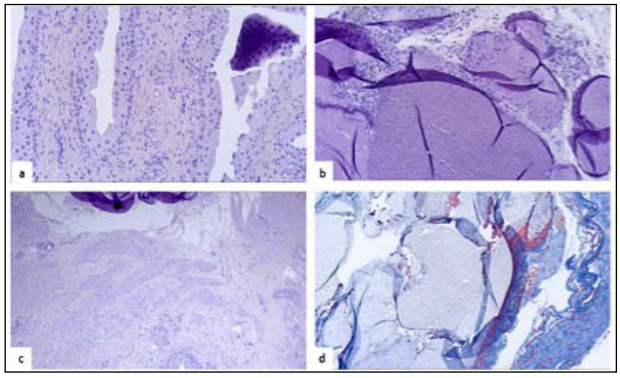

metaplasia, dysplasia, or cellular atypia was observed. The inflammatory response of the urothelium was minimal: polymorphonuclear leukocytes, lymphocytes, and plasma cells were absent, and no multinucleated giant-cell infiltration was detected.
The lamina propria showed no signs of fibrosis or pathological neovascularization. Occasional lymphocytes and multinucleated giant cells were identified in isolated areas (0-0.25 points). The muscular layer preserved its structural integrity without signs of inflammation, fibrosis, or sclerosis.
A thin fibrous capsule was formed in all samples (100%), clearly delineating the implant from the surrounding tissues. Collagen fibers were arranged in parallel bundles; capsule thickness was rated at 1 (1-1) point, and collagen density and fibrosis at 1 (1-1.25) points, indicating a moderately expressed connective tissue barrier without evidence of marked sclerosis or hyalinization. The cellular composition consisted mainly of fibroblasts and occasional macrophages (≤ 5 cells per 5 high-power fields, ×200 magnification). Lymphocytic and macrophagic infiltration remained minimal. The multinucleated giant-cell reaction did not exceed 1 point, confirming favorable biocompatibility of the material and the absence of a pronounced foreign-body response.

aesPLLa, Day 90
At 90 days after implantation of aesPLLa into the urinary bladder, histological examination revealed signs of material biodegradation accompanied by minimal vascularization and stable tissue regeneration (Table 1, Figure 12). The urothelium and adjacent lamina propria exhibited moderate inflammatory alterations characterized by eosinophilic infiltration, edema, and vascular congestion, indicative of a localized immune response.
Histologically, the urothelium displayed structural changes, including epithelial thinning, desquamation, and disruption of intercellular junctions with focal erosions (median score 1 [1-2]). In all samples (100%), pathological alterations of cellular organization were noted, manifested as loss of stratification, cytoplasmic dystrophy, and vacuolization (median score 1 [1-1]). The inflammatory infiltrate was dominated by eosinophils (3 [3-3]), suggesting a hypersensitivity-type response, while lymphocytic infiltration was mild (0.5 [0-1]). Polymorphonuclear neutrophils and multinucleated giant cells were absent.
The lamina propria consisted of loose connective tissue without signs of fibrosis or pathological neovascularization. Occasional lymphocytes and plasma cells were observed (0.5 [0-1]) in the absence of neutrophilic or eosinophilic infiltration.
The muscular layer maintained its morphological integrity and normal orientation of smooth muscle fibers without evidence of inflammation, fibrosis, or sclerosis. Moderate interstitial edema and focal lymphocytic infiltration were present, though no severe dystrophic changes were detected.
Formation of a fibrous capsule around the implant was not observed. Collagen fibers did not exhibit compaction, thickening, or sclerotic remodeling.
Thus, by day 90, residual aesPLLa fragments were detected within the lamina propria as evenly distributed violet-blue strands surrounded by loose connective tissue, without evidence of pronounced inflammation or fibrotic reaction.

Figure 12.
aesPLLa group at day 90.

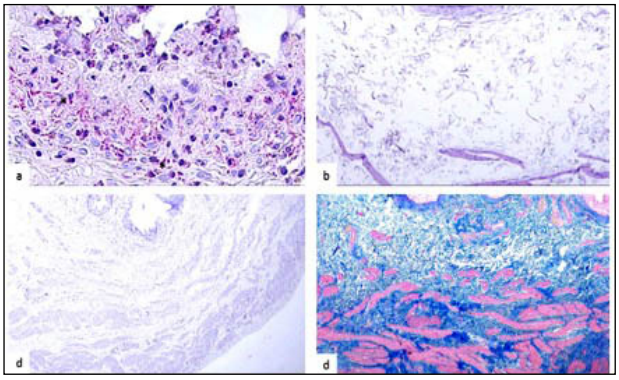

Polyacrylate and polyvinyl alcohol copolymer, Day 90
At 90 days after implantation of polyacrylate and polyvinyl alcohol copolymer into the urinary bladder wall, the implant partially persisted, appearing as compact, homogeneous masses surrounded by a thin fibrous capsule (Table 1, Figure 13). The material exhibited structural stability and high biocompatibility, without eliciting a pronounced inflammatory response or diffuse fibrosis. Only minimal tissue alterations were observed, including the formation of a delicate fibrous capsule and moderate vascularization of the lamina propria.
The urothelial layer remained structurally intact in six (75%) cases, while mild focal hyperplasia was observed in two (25%) specimens, with a median score of 0.5 (0-1). Cellular composition and epithelial organization remained within normal limits in five (62.5%) cases, with only minor stratification irregularities, cytoplasmic dystrophy, or vacuolization detected in some samples.
No inflammatory response was observed in the urothelium: polymorphonuclear neutrophils, eosinophils, lymphocytes, and plasma cells were absent. Metaplasia, dysplasia, and cytological atypia were not detected in any of the examined specimens (100%).
The lamina propria exhibited preserved histoarchitecture without signs of fibrosis or pathological neovascularization. Inflammatory infiltration was minimal, represented by occasional lymphocytes and multinucleated giant cells

Table 1.
Histopathological evaluation of epithelial, lamina propria, and muscular layer alterations in the rabbit urinary bladder 90 days after implant administration.

N.	Parameters	Group I Autologous fat graft (n = 8)	Group II PRP + Autologous fat graft (n = 8)	Group III aesPLLa (n=8)	Group IV Polyacrylate and polyvinyl alcohol copolymer (n = 8)
I.	**Epithelium**				
1.	Structural integrity				
	Normal, n (%)	8 (100)	8 (100)	0 (0)	6 (75)
	Pathology (desquamation, thinning, hyperplasia, or erosion)	0	0	1 (1-2)	0.5 (0-1)
2.	Cell composition and organization				
	Normal, n (%)	5 (62.5)	7 (87.5)	0 (0)	5 (62.5)
	Pathology (loss of stratification, dystrophy, cellular vacuolization)	0 (0-1.25)	0	1 (1-1)	0 (0-1)
3.	Inflammation				
	Polymorphonuclear neutrophils	0	0	0	0
	Eosinophils	0	0	3 (3-3)	0
	Lymphocytes and plasma cells	0	0	0.5 (0-1)	0
	Multinucleated giant cells	0	0	0	0
4.	Metaplasia				
	Present, n (%)	0 (0)	0 (0)	0 (0)	0 (0)
	Absent, n (%)	8 (100)	8 (100)	8 (100)	8 (100)
5.	Dysplasia or atypia				
	Present, n (%)	0 (0)	0 (0)	0 (0)	0 (0)
	Absent, n (%)	8 (100)	8 (100)	8 (100)	8 (100)
II.	**Lamina propria**				
1.	Fibrosis	2 (2 -2.25)	1 (0-1)	0	0
2.	Vascularization	0	1 (0.75-1)	0	0
3.	Inflammation				
	Polymorphonuclear neutrophils	0	0	0	0
	Eosinophils	0	0	0	0
	Lymphocytes and plasma cells	1 (0-1)	0.5 (0-1)	0.5 (0-1)	0 (0-0.25)
	Multinucleated giant cells	1 (0-1)	1 (0-1)	0	0 (0-0.25)
III.	**Muscular layer**				
1.	Fibrosis and sclerosis	0	0	0	0
2.	Inflammation	0	0	0	0
IV.	**Capsule around the implant**				
	Absent, n (%)	1 (12.5)	0	8 (100)	0
	Present, n (%)	7 (87.5)	8 (100)	0	8 (100)
	Capsule thickness	2 (1-2)	1 (1-1.25)	0	1 (1-1)
	Cellular composition	1 (1-1.25)	1.5 (1-2.25)	0	1 (1-1)
	Fibrosis and collagen density	2 (1.75-2)	2 (1-2)	0	1 (1-2)
	Inflammation	1 (0-1.25)	1 (1-1)	0	1 (1-1.25)
	Giant cell reaction	1 (0.75-1)	1 (1-1.25)	0	1 (1-1)

Figure 13.
Vantris group at day 90.

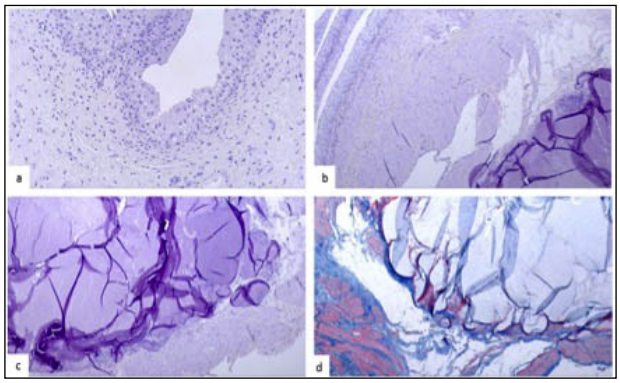

(score 0-0.25). The muscular layer retained normal morphology, showing no evidence of fibrosis, dystrophy, or inflammatory infiltration.

In all specimens (100%), a thin fibrous capsule formed around the implant. The mean capsule thickness was 1 (1-1), corresponding to a moderately developed capsule. The cellular composition consisted predominantly of fibroblasts and sparse macrophages (≤ 5 cells per 5 high-power fields at ×200 magnification), with an inflammatory score of 1 (1-1). The capsule was composed of collagen bundles with focal thickening of fibers but no signs of extensive fibrosis. Inflammation within the capsule was minimal, estimated at 1 (1-1.25) points, reflecting mild lymphocytic and macrophage infiltration (≤ 5 cells per 5 fields at ×200). Rare multinucleated giant cells (1-4 cells per 5 fields at ×200) were also observed.

Thus, polyacrylate and polyvinyl alcohol copolymer maintained a dense and homogeneous structure, indicating material stability and slow biodegradation. The implant was encapsulated by a thin fibrous layer clearly delineating it from the surrounding tissues, confirming adequate tissue adaptation without evidence of excessive remodeling or hyperplasia.

Comparative assessment of graft survival, structural stability, and morphological characteristics

Figure 14 presents photographs of bladder tissues with implanted materials on day 90 post-implantation, while Table 2 illustrates a comparative assessment of graft survival, structural stability, and morphological integrity of the implants.

Group I - Autologous fat graft (n = 8)

Upon analysis of implant migration, no displacement was observed in 2 cases (25%), minimal displacement in 4 cases (50%), moderate displacement in 1 case (12.5%), and marked displacement in 1 case (12.5%). The mean score was 1.88 ± 0.83.

In 7 cases (87.5%), the bolus exhibited a rounded and symmetrical morphology, while in 1 case (12.5%) it appeared oval and slightly elongated, reflecting a satisfactory degree of structural stability of the material. The mean score was 2.88 ± 0.35.

By day 14 post-implantation, assessment of implant survival demonstrated moderate volume reduction (30-50%) in 25% of cases and substantial reduction (> 50%) in 75% of cases. Complete resorption was consistently associated with fibrosis and cellular infiltration (100% of samples), indicating limited biostability of the autologous fat graft. The mean score was 1.25 ± 0.46.

Figure 14.
Bladder tissues with implant materials at day 90 after implantation.

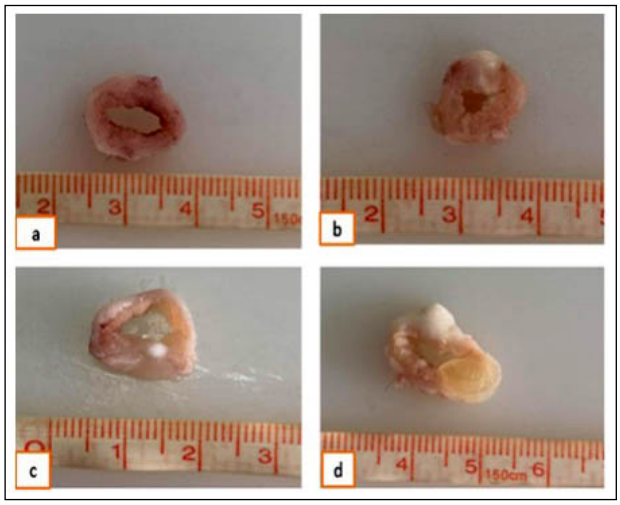

a. Autologous fat graft; b. PRP-enhanced autologous fat graft; c. aesPLLa; d. Vantris.

Group II - PRP-enhanced autologous fat graft (n = 8)

Analysis of implant migration revealed no displacement beyond the target area (0%). Absence of migration was observed in 3 cases (37.5%), minimal displacement in 2 cases (25%), and moderate displacement in 3 cases (37.5%). These findings indicate sufficient positional stability of the implant; however, the presence of moderate migration in more than one-third of cases may reflect uneven distribution of the material within the implantation zone. The mean score was 2.00 ± 0.93, demonstrating considerable variability across samples.

Table 2.
Comparative characteristics of implant migration within the bladder wall, bolus morphology, uniformity of implant distribution, and survival at 90 days

N.	Parameters	Group I Autologous fat graft (n = 8)	Group II PRP + Autologous fat graft (n = 8)	Group III aesPLLa (n=8)	Group IV Polyacrylate and polyvinyl alcohol copolymer (n = 8)
1	**Migration (implant displacement)**				
	No displacement	2 (25)	3 (37.5)	0 (0)	3 (37.5)
	Minimal displacement	3 (37.5)	2 (25)	1 (12.5)	3 (37.5)
	Moderate displacement	3 (37.5)	3 (37.5)	7 (87.5)	2 (25)
	Marked displacement or migration beyond organ boundaries	-	-	-	-
	Score, M ± SD	1.88 ± 0.83	2.00 ± 0.93	1.13 ± 0.35	2.13 ± 0.35
2	**Bolus shape**				
	Round, symmetrical	7 (87.5)	6 (75)	-	1 (12.5)
	Oval, elongated	1 (12.5)	2 (25)	-	7 (87.5)
	Irregular / other	-	-	8 (100)	-
	Not defined	-	-	-	-
	Score, M ± SD	2.88 ± 0.35	2.75 ± 0.46	1.0 ± 0.0	2.13 ± 0.35
3	**Bolus volume preservation**				
	Significant volume preservation (>50%)	-	3 (37.5)	-	6 (75)
	Moderate volume preservation (30-50%)	2 (25)	5 (62.5)	1 (12.5)	2 (25)
	Minimal volume preservation (<30%)	6 (75)	-	7 (87.5)	-
	No preservation	-	-	-	-
	Score, M ± SD	1.25 ± 0.46	2.38 ± 0.52	1.88 ± 0.35	2.75 ± 0.46
	Integrated survival index	66.7	79.2	44.4	77.8

A rounded and symmetrical bolus configuration was observed in 6 cases (75%), whereas in 2 cases (25%) the shape appeared oval and slightly elongated. Such morphological characteristics suggest an adequate degree of structural organization of the PRP-autologous fat composite, although in one-quarter of cases the bolus deviated from the optimal form. The mean score was 2.75 ± 0.46, indicative of a high quality of spatial material distribution.
Uniformity of implant distribution was noted in 100% of cases, with compact localization of the graft material confirming its good retention within the implantation area.
Evaluation of implant survival at day 14 demonstrated minimal volume reduction (< 30%) in 3 cases (37.5%) and moderate reduction (30-50%) in 5 cases (62.5%). Complete resorption was not observed in any sample, indicating satisfactory biostability of the PRP-autologous fat graft. The mean score was 2.38 ± 0.52.

Group III - aesPLLa (poly-L-lactic acid) (n = 8)
Analysis of implant migration parameters revealed that displacement of varying degrees was observed in all 8 cases (100%): minimal in 2 cases (25%), moderate in 5 cases (62.5%), and pronounced or extra-organ displacement in 1 case (12.5%). The mean migration score was 1.13 ± 0.35.
The bolus configuration was characterized by a diffuse and disordered distribution of the material among connective tissue fibers in all cases (100%), indicating insufficient localization of the implant within the target area. The mean histomorphometric score was 1.0 ± 0.0.
Assessment of implant survival at day 14 demonstrated substantial volume reduction or complete resorption in 7 cases (87.5%), while moderate volume reduction (30-50%) was observed in 1 case (12.5%). In all instances of complete resorption, tissue architecture returned to normal morphology without evidence of fibrosis, inflammation, or cellular infiltration. The mean implant survival score was 1.88 ± 0.35.

Group IV - Polyacrylate and polyvinyl alcohol copolymer (n = 8).
Absence of implant displacement was recorded in 3 cases (37.5%), minimal displacement in 3 cases (37.5%), and moderate to pronounced displacement in 1 case (12.5%). The mean histomorphometric migration score was 2.13 ± 0.35.
In 7 cases (87.5%), the bolus exhibited an oval, slightly elongated configuration, whereas in 1 case (12.5%) it appeared rounded and symmetrical with a well-defined spatial organization of the material. The mean morphology score was 2.13 ± 0.35.
Evaluation of implant survival at day 14 revealed minimal volume reduction (< 30%) in 6 cases (75%) and moderate reduction (30-50%) in 2 cases (25%). No instances of complete material resorption were observed. The mean survival score was 2.75 ± 0.46.
Collectively, the most stable materials in terms of positional fixation and shape retention were polyacrylate and polyvinyl alcohol copolymer and PRP-enhanced autologous fat graft, where marked or significant displacement was extremely rare, and the bolus morphology remained predominantly rounded and symmetrical. In contrast, aesPLLa implants demonstrated the least spatial stability and shape preservation, characterized by diffuse and disorganized material distribution.
Implant survival varied substantially depending on the material composition. Polyacrylate and polyvinyl alcohol copolymer and PRP-autologous fat grafts showed the highest resistance to resorption, while aesPLLa and autologous fat grafts exhibited marked volume loss or complete resorption.
Based on these findings, PRP-autologous fat graft and polyacrylate and polyvinyl alcohol copolymer demonstrate superior spatial fixation, morphological stability, and volume preservation, indicating their potential as promising candidates for further clinical application.

Discussion

In the course of an experimental study conducted on 96 rabbits, a comparative morphofunctional evaluation of volume-forming materials of different origins was performed following their implantation into the submucosal layer of the urinary bladder. It was established that the combination of autologous fat grafting with platelet-rich plasma (PRP) and the synthetic material polyacrylate and polyvinyl alcohol copolymer demonstrated the most favorable outcomes in terms of biocompatibility, structural stability, and implant survival throughout the 90-day observation period.
Polyacrylate and polyvinyl alcohol copolymer maintained its volumetric effect throughout the entire experimental period (Figure 15), demonstrating the formation of a well-defined fibrous capsule, the absence of pronounced inflammatory infiltration (Figure 16), and a clearly delineated intramural localization of the bolus. Histological examination revealed a moderate fibrotic response and uniform distribution of the material within the submucosal and deeper layers, which correlated with a high degree of structural stability.

Figure 15.
Preservation of implant volume across study groups.

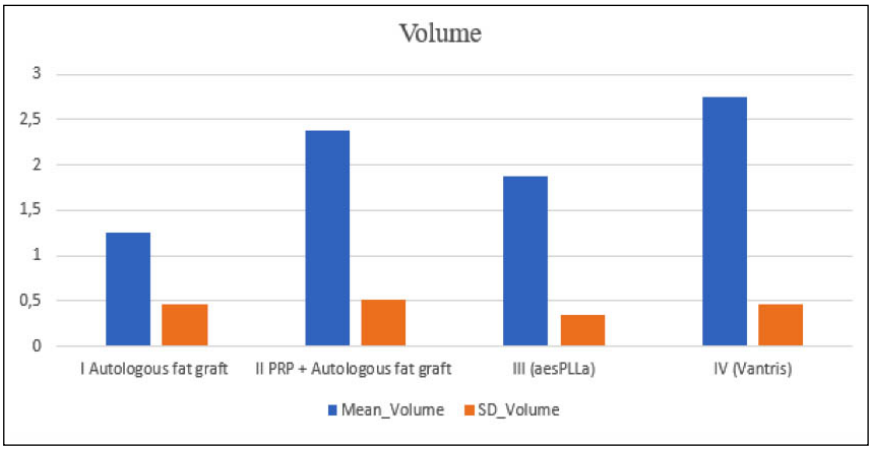

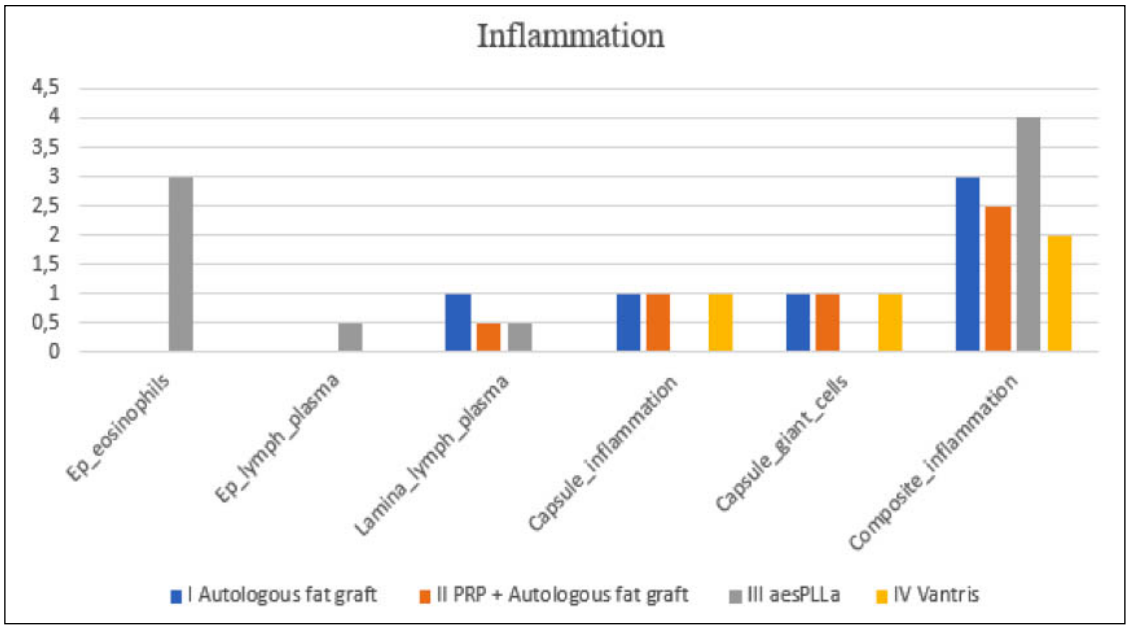

Figure 16. *Inflammatory response patterns across study groups.*

The combination of PRP with autologous fat grafting markedly improved adipose tissue survival compared to isolated lipotransplantation. According to morphometric analysis, the mean retained graft volume at day 90 was 72.3%, *versus* 41.5% in the group receiving fat alone. In the PRP + fat group, there were no signs of active inflammation, allergic or necrotic reactions, while evidence of angiogenesis and the formation of a connective tissue capsule ensuring material fixation was observed. These findings are consistent with published data highlighting the role of PRP in enhancing tissue repair and attenuating inflammatory response (22, 23, 24).

The aesPLLa material demonstrated the poorest performance among the evaluated samples. By day 90, extensive resorption was observed, with less than 10% of the initial volume remaining. No capsule formation was detected, and the material exhibited marked diffusion within the submucosal layer, accompanied by moderate eosinophilic infiltration. The pronounced migration, weak collagenization, and lack of well-defined implant boundaries indicate poor tissue integration and insufficient mechanical fixation, particularly within the loose connective tissue of the rabbit bladder wall, which lacks a distinct collagen framework.

Overall analysis indicated that the degree of implant migration varied according to the type of material. The highest mobility was observed with aesPLLa, moderate mobility in the autologous fat graft group, and minimal displacement in the polyacrylate and polyvinyl alcohol copolymer and PRP + fat groups. Bolus morphology also differed: rounded in the fat and PRP groups, and elongated with ill-defined boundaries in the aesPLLa group.

Importantly, none of the materials tested induced signs of invasive growth, disruption of the urothelial lining, or pathological tissue transformation, indicating their relative biocompatibility under short-term observation.

In conclusion, the present findings indicate the high efficacy and biocompatibility of the combination of PRP with autologous fat grafts and the Vantris material, identifying them as the most promising approaches for achieving a stable volumetric effect in urological applications. In contrast, the use of biodegradable polymers such as aesPLLa requires caution due to their low stability and limited tissue integration. The prospects for clinical implementation of the inves-

Declarations

Ethical approval and consent for participate: *The protocol for the blinded randomized in vivo study was approved by the Bioethics Committee of the Non-profit Joint Stock Company "Karaganda Medical University" (Protocol No. 91, dated December 3, 2024). All experimental procedures were conducted in accordance with the ethical principles for animal research and under the supervision of a certified veterinarian to prevent any unnecessary pain, distress, or suffering throughout the study.*

Competing interests: *The authors declare that they have no competing interests.*

Availability of data and material: *All data generated or analyzed during this study are available upon request.*

Funding: *His article receives no financial support.*

Authors' contributions: *Askarov M.S. – conceptualization, supervision, retrospective data organization, manuscript review; Pak I.L. – critical revision of the draft, approval of the final version;Yeskermessov D.B. – literature search, data collection, statistical analysis, drafting of the manuscript; Batenova U.G. – data processing, drafting of the manuscript; descriptive analysis; Klyuyev D.A. – supervision, formal analysis; Kamyshanskiy Y.K. – supervision, approval of the final version; Min Sung Tak – supervision, approval of the final version.*

Acknowledgments: *I would like to express my deepest gratitude to my scientific supervisors – Askarov M.S., Pak I.L., Klyuyev D.A., and Kamyshanskiy Y.K. – for their invaluable guidance, insightful advice, and unwavering support throughout the entire course of this work. My sincere appreciation is also extended to my co-authors for their invaluable contributions to the development of the manuscript. Their meticulous work and thoughtful input have significantly enhanced the overall quality of this study.*

tigated materials warrant further validation through extended preclinical and clinical studies with prolonged follow-up and functional assessment of bladder integrity.

Conclusions

Thus, the combination of autologous fat with PRP demonstrates efficacy comparable to that of synthetic materials, providing a high degree of biocompatibility and volume retention. Moreover, autologous fat with PRP represents a fully accessible and cost-free material that does not elicit immune responses, making it a promising alternative to synthetic implants in reconstructive urology.

References

1. Serati M, Braga A, Vitelli A, et al. Urethral bulking agents for the treatment of recurrent stress urinary incontinence: A systematic review and meta-analysis. Int Urogynecol J. 2022; 33:1137-1146.

2. Oguz F, Yildiz T, Gecit I, et al. The outcomes of two different bulking agents (dextranomer hyaluronic acid copolymer and polyacrylate polyalcohol copolymer) in the treatment of primary vesicoureteral reflux. Int Braz J Urol. 2016; 42:514-520.

3. Bozacı AC, Aki FT, Zeybek D, et al. Comparison of the histological response to different bulking materials used in endoscopic vesicoureteral reflux surgery. Bagcilar Med Bull. 2022; 9:117-123.

4. Sharifiaghdas F, Narouie B, Soltani MH, et al. Investigating the clinical outcomes of bulking agent injection in comparison with modified Gil Vernet anti-vesicoureteral reflux surgery in children with high-grade reflux (4 or 5). Afr J Urol. 2023; 29:67.

5. Vasudeva P, Yadav S, Sinha S, et al. Autologous versus synthetic midurethral transobturator sling: A systematic review and meta-analysis of outcomes. Neurourol Urodyn. 2024; 43:2017-2029.

6. Kuismanen K, Kaestel M, Seiler R, et al. Autologous adipose stem cells in treatment of female stress urinary incontinence: Results of a pilot study. Stem Cells Transl Med. 2014; 3:315-321.

7. Daneshpajooh A, Farsinejad A, Derakhshani A, et al. Comparing periurethral injection of autologous muscle-derived stem cells and fibroblasts with midurethral sling surgery in the treatment of female stress urinary incontinence: A randomized clinical trial. J Stem Cells Regen Med. 2022; 18:43-51.

8. Legonkova OA, Sultanova NO, Stafford VV, et al. Long-term biodegradation of polyacrylamide gel residues in mammary glands: Physicochemical analysis, chromatographic detection, and implications for chronic inflammation. Molecules. 2024; 29:3247.

9. Carey JM, Chon JK, Leach GE. Urethrolysis with Martius labial fat pad graft for iatrogenic bladder outlet obstruction. Urology. 2003; 61:21-25.

10. Inoyatov JS, Snurnitsyna OV, Lobanov MV, et al. Minimally invasive combined surgical treatment of postcoital cystitis. Andrology and Genital Surgery. 2020; 21:20-25.

11. Alshuaibi M, Zugail AS, Lombion S, Beley S. New protocol in the treatment of Peyronie's disease by combining platelet-rich plasma, percutaneous needle tunneling, and penile modeling: Preliminary results. Fr J Urol. 2024; 34:102526.

12. Cirigliano L, Di Giovanni A, Giordano A, et al. Hyaluronic acid injection for the management of Peyronie's disease. J Sex Med. 2022; 19: S16.

13. Casavantes L, Lemperle G, Morales P. Penile girth enhancement with polymethylmethacrylate-based soft tissue fillers. Aesthet Surg J. 2016; 36:1414-1422.

14. Ministry of Health of the Republic of Kazakhstan. Order No. KR DSM-248/2020 dated December 11, 2020. On approval of the rules for conducting clinical trials of medicinal products and medical devices. Available from: https://adilet.zan.kz/rus/docs/V2000021772 /info (Accessed: 2022 Apr 2).

15. Ministry of Health and Social Development of the Republic of Kazakhstan. Good Laboratory Practice (GLP) Standard. Order No. 392 dated May 27, 2015. Available from: https://adilet.zan.kz/rus/ docs/V1500011506 (Accessed: 2022 Apr 19).

16. Council of Europe. European Convention for the Protection of Vertebrate Animals used for Experimental and Other Scientific Purposes. Strasbourg, 18.III.1986. Available from: https:// rm.coe.int/168007a67b (Accessed: 2023 Feb 2).

17. Allgoewer A, Mayer B. Sample size estimation for pilot animal experiments by using a Markov Chain Monte Carlo approach. Altern Lab Anim. 2017; 45:83-90.

18. Hersant B, Bouhassira J, SidAhmed-Mezi M, et al. Should platelet-rich plasma be activated in fat grafts? An animal study. J Plast Reconstr Aesthet Surg. 2018; 71:681-690.

19. Dupras J, Vachon P, Cuvelliez S, Blais D. Anesthesia of the New Zealand rabbit using the combination of tiletamine-zolazepam and ketamine-midazolam with or without xylazine. Can Vet J. 2001; 42:455-460.

20. Pak I, Askarov M, Kissamedenov N, Klyuyev D, Kamyshanskiy Y. Experimental study on clinical and morphological determination of the optimal cannula diameter for lipoaspirate harvest from rabbit inguinal fat pad. J Appl Biomed. 2023; 21:99-105.

21. International Organization for Standardization. Biological evaluation of medical devices - Part 6: Tests for local effects after implantation. ISO/DIS 10993-6:2024.

22. Liao HT, Marra KG, Rubin JP. Application of platelet-rich plasma and platelet-rich fibrin in fat grafting: Basic science and literature review. Tissue Eng Part B Rev. 2014; 20:267-276.

23. Xiong BJ, Tan QW, Chen YJ, et al. The effects of platelet-rich plasma and adipose-derived stem cells on neovascularization and fat graft survival. Aesthet Plast Surg. 2018; 42:1-8.

24. El-Sharkawy H, Kantarci A, Deady J, et al. Platelet-rich plasma: Growth factors and pro- and anti-inflammatory properties. J Periodontol. 2007; 78:661-669.

Correspondence

Meirambek Askarov - askarov@qmu.kz
Ilona Pak - dr.park@bk.ru
Department of Surgical Diseases, Karaganda Medical University, Karaganda, Kazakhstan

Dauren Yeskermessov (Corresponding Author)
eskermesov.dauren@mail.ru
Ulpan Batenova - batenovaulpan@gmail.com
Dmitriy Klyuyev - klyuyev@qmu.kz
Institute of Life Sciences, Karaganda Medical University, Karaganda, Kazakhstan

Yevgeniy Kamyshanskiy - kamyshanskiy@qmu.kz
Head of the Pathological Anatomy Unit of the Clinic of Karaganda Medical University, Karaganda, Kazakhstan

Min Sung Tak - tarkms@naver.com
Department Plastic Surgery, Soon Chun Hyang University Cheonan Hospital, Cheonan, South Korea